



1     **Estimation of CFC-11 emissions from coal combustion in China**

2

3     Zhenzhen Niu <sup>1</sup>, Shaofei Kong <sup>1,2\*</sup>, Qin Yan <sup>1</sup>, Yi Cheng <sup>1</sup>, Huang Zheng <sup>1</sup>, Yao Hu <sup>1</sup>,  
4     Jian Wu <sup>1,2</sup>, Xujing Qin <sup>1</sup>, Haoyu Dong <sup>1</sup>, Weisi Jiang <sup>1</sup>, Yingying Yan <sup>1</sup>, Wei Liu <sup>3</sup>,  
5     Feng Ding <sup>3</sup>, Yongqing Bai <sup>4</sup>, Shihua Qi <sup>1,2</sup>

6

7     <sup>1</sup> Department of Atmospheric Sciences, School of Environmental Studies, China  
8     University of Geosciences (Wuhan), Wuhan, 430078, China

9     <sup>2</sup> Research Centre for Complex Air Pollution of Hubei Province, Wuhan, 430078,  
10     China

11     <sup>3</sup> Hubei Province Academy of Eco-Environmental Sciences, Wuhan, 430072, China

12     <sup>4</sup> Institute of Heavy Rain, China Meteorological Administration, Wuhan, 430205,  
13     China

14     \* Corresponding to Shaofei Kong ([kongshaofei@cug.edu.cn](mailto:kongshaofei@cug.edu.cn))

15



## 16 Abstract

17 The trichlorofluoromethane (CFC-11) emission from its production and use  
18 (PAU) has drawn wide attention, while its combustion sources have been overlooked.  
19 This study identified CFC-11 emission factors (EFs) as 3.6, 3.2, and 0.025 mg kg<sup>-1</sup>  
20 from the combustion of domestic chunk coal, honeycomb briquette, and coal-fired  
21 power plant, respectively. A multi-year (2000~2021) emission inventory of CFC-11  
22 from coal combustion was established in China. Results indicated that its annual  
23 emission averaged 233.5 t yr<sup>-1</sup>. It exhibited fluctuations and held an overall upward  
24 trend, increasing from accounting for 0.8% of PAU emissions in 2000 to 9.8% in 2021,  
25 with the peak value appearing in 2016. In Shandong and Hebei provinces with high  
26 coal consumption amounts, the CFC-11 emissions from coal combustion increased by  
27 approximately 74% during 2014~2017 compared to 2011~2012. At the Gosan station  
28 close to Chinese mainland, CFC-11 emitted from coal combustion in Hebei and  
29 Shandong was approximately occupied by ~30% of its average concentration during  
30 January 2016. An additional climate effect of the clean heating and coal-to-electricity  
31 policies in China was also observed, with an obvious decrease ( $2.2 \times 10^6$  t and  $3.4 \times 10^7$   
32 t) of CO<sub>2</sub>-equivalent emission. This study provides substantial evidence of CFC-11  
33 emission from coal combustion and highlights the role of combustion emission under  
34 the background of reducing CFC-11 from PAU. The data compiled in this work can  
35 found at <https://doi.org/10.6084/m9.figshare.28523063> (Niu et al., 2025).

36

37 **Keywords:** Coal combustion; Trichlorofluoromethane emissions; Emission inventory;  
38 Global warming potential; WRF-FLEXPART simulation



## 39 1. Introduction

40 Trichlorofluoromethane (CFC-11) has been widely used as a blowing agent for  
41 foams incorporated into buildings and consumer products since the 1950s (McCulloch  
42 et al., 2001; Rigby et al., 2019). The lifetime of CFC-11 exceeds 50 years, allowing it  
43 to accumulate in the atmosphere (Guo et al., 2009; Lickley et al., 2021; Rigby et al.,  
44 2013). CFC-11 could deplete stratospheric ozone through photodissociation (Fleming  
45 et al., 2020; Molina & Rowland, 1974), and served as a reference compound for  
46 calculating ozone depletion potential (ODP) (Western et al., 2023). Over a 100-year  
47 time horizon, CFC-11 has a global warming potential (GWP) thousands of times  
48 greater than that of carbon dioxide (CO<sub>2</sub>) (Chiodo & Polvani, 2022; Polvani et al.,  
49 2020). An accurate understanding of CFC-11 emissions was helpful for assessing the  
50 impact of China's implementation of the Montreal Protocol (Fang et al., 2018).

51 The production and consumption of CFC-11 for emissive applications were  
52 phased out globally in 2010 according to the Montreal Protocol released in 1987 (Park  
53 et al., 2021). It results in a declining trend of its global atmospheric concentration  
54 (Park et al., 2021), and an expectation for ozone-layer recovery throughout the 21st  
55 century (Scientific assessment of ozone depletion, 2019). However, since 2012, the  
56 decline rate of atmospheric CFC-11 emission has significantly slowed by about 50%  
57 (Montzka et al., 2018). Eastern China has been identified as a hotspot for unexpected  
58 increased emissions of CFC-11 (Park et al., 2021). Former studies attributed it to new  
59 productions of CFC-11 in Eastern China (Montzka et al., 2018; Rigby et al., 2019),  
60 especially for blowing closed-cell insulating foam (McCulloch et al., 2001). Based on  
61 ambient monitoring data, former studies simulated CFC-11 emissions increased by  
62 29.4% globally (Montzka et al., 2021), 58.3% in East Asia (Adcock et al., 2020), and  
63 130.7% in eastern China (Park et al., 2021) during 2014~2017 compared to  
64 corresponding values of 2011~2012. They concluded that the annual emissions from  
65 existing CFC-11 banks alone could not fully explain the observed increase,  
66 highlighting a need to evaluate other potential sources for unexpected emissions



67 (Montzka et al., 2018). Therefore, the identification of new CFC-11 emission sources  
68 and updating its emission estimation are urgent works.

69 There are two popular methods frequently adopted to estimate CFC-11 emissions.  
70 The first was estimating its emissions based on atmospheric observation dataset,  
71 including the inverse modeling approach which identified the CFC-11 emission using  
72 two backward-running Lagrangian models, the UK Met Office Numerical  
73 Atmospheric-dispersion Modelling Environment (NAME) and the FLEXible  
74 PARTicle dispersion model (FLEXPART) (Park et al., 2021), and ratio method which  
75 according to a correlation of CFC-11 with tracers holding clear emissions (Zhang et  
76 al., 2014). Many tracers were adopted in former studies, such as carbon monoxide  
77 (CO), chloroform (CHCl<sub>3</sub>), and carbon tetrachloride (CCl<sub>4</sub>) (Adcock et al., 2020;  
78 Huang et al., 2021). CO was widely selected as its emission inventory was established  
79 well and updated frequently by MEIC (Multiresolution Emission Inventory for China,  
80 <http://meicmodel.org.cn/#firstPage>). The essential precondition is that the CFC-11 and  
81 CO sources were co-located (Dhomse et al., 2019; Huang et al., 2021; Kim et al.,  
82 2010). However, CO is a tracer for incomplete combustion (Zeng et al., 2020). If the  
83 CFC-11 emission amounts were obtained by multiplying CO emission amounts with a  
84 CFC-11/CO ratio from a linear fit, the results were untenable for the following two  
85 reasons: (1) CFC-11/CO ratios selected varied in different researches, as 0.087  
86 (Huang et al., 2021), 0.079 (Huang et al., 2021), 0.027~0.069 (Palmer et al., 2003),  
87 and 0.022 (Shao et al., 2011). There was no objective criterion for selecting the CFC-  
88 11/CO ratios. (2) The hypothetical co-locations of CFC-11 and CO do not mean that  
89 their sources are the same. The obtained CFC-11 emission amounts through this  
90 method actually mean that CFC-11 is only related to combustion sources.

91 The second was a bottom-up method. The CFC-11 emission inventory was  
92 estimated based on the reported CFC-11 production and use (PAU) amounts from  
93 different sectors, including foam blowing, solvents, and refrigerators (Fang et al.,  
94 2018; Wan et al., 2009; Zhao et al., 2011), and combustion sources were always not



95 included. Additionally, in the fields of source profiles of volatile organic compounds  
96 (VOCs), CFC-11 has been frequently detected for various types of combustion  
97 sources (Gong et al., 2019; SPECIATE Version 5.3; Sha et al., 2021; Sun et al., 2019)  
98 The emitted mass concentrations or emission factors of CFC-11 from various  
99 combustion sources have also widely reported, such as power plant ( $12.5 \mu\text{g m}^{-3}$ ) (Shi  
100 et al., 2015), gasoline and diesel vehicles ( $0.01\sim0.06 \text{ mg km}^{-1}$ ) (Wang et al., 2020),  
101 and coal combustion ( $0.07\sim0.51 \text{ ppbv}$ ) (Li et al., 2003). CFC-11 can be formed by the  
102 combustion of coal that contains the necessary elements of carbon, chlorine, and  
103 fluorine (Jin et al., 2025; Luo et al., 2004). The level of CFC-11 has been detected at  
104 ppb levels in combustion (Pons et al., 2019), which is 3 magnitudes higher than its  
105 ambient levels. To the best of our knowledge, the emission inventory of CFC-11  
106 emissions from combustion sources has not been reported.

107 To sum up, we detected the emission factors (EFs) of CFC-11 from domestic  
108 coal combustion (chunk coal and honeycomb briquette) and coal-fired power plants  
109 with a unified dilution sampling method. An emission inventory with high spatial  
110 resolution of CFC-11 from coal combustion in China during 2000~2021 was first  
111 established. The variation trends of CFC-11 emitted from coal combustion and PAU  
112 were compared. The impact of CFC-11 emissions from coal combustion in the  
113 hotspots of Shandong and Hebei provinces on coastal air was simulated with the  
114 WRF-FLEXPART model. This study provides a quantitative assessment of CFC-11  
115 emissions from coal combustion in China, which will provide new insights for  
116 identifying its variation trend in ambient air and refining the projection of  
117 stratospheric ozone layer recovery.

## 118 2. Methods

### 119 2.1 Source sampling

120 To ensure the representativeness and applicability of the emission factors, the  
121 combustion experiments were designed to closely simulate real-world domestic coal  
122 combustion conditions in rural China. A total of 10 kinds of chunk coals and 11 kinds



123 of honeycomb briquettes were collected and burned in our combustion lab in Wuhan.  
124 The annual average ambient level of CFC-11 was  $0.6 \mu\text{g m}^{-3}$  in the year 2023. Fuels  
125 were collected from eight agricultural regions of China, including the Northeast Plain  
126 (Heilongjiang, Jilin, and Liaoning), Arid and semi-arid regions of north China (Inner  
127 Mongolia, Ningxia, Gansu, and Xinjiang), Loess Plateau (Shaanxi and Shanxi), North  
128 China plain (Anhui, Beijing, Hebei, Henan, Jiangsu, Shandong, Shanghai and Tianjin),  
129 Yangtze Plain (Hubei, Hunan, Jiangxi, and Zhejiang), Sichuan Basin (Sichuan and  
130 Chongqing), Yunnan-Guizhou Plateau (Guangxi, Guizhou, and Yunnan), Tibet Plateau  
131 (Qinghai and Xizang) and South China (Fujian, Guangdong, and Hainan). The  
132 specific information on fuel collection can be seen in Table S1. If the fuel in one  
133 region had not been collected, the fuel emission characteristics of the neighboring  
134 provinces were used as a substitute.

135 The stove used was a typical household furnace purchased from a local market,  
136 with an outer diameter, inner diameter, and height of 30, 12, and 43 cm, respectively.  
137 For each test, about 0.8 kg chunk coals and 1.5 kg honeycomb briquettes (three pieces)  
138 were burned. The combustion process was manually operated to replicate the real  
139 usage patterns of rural households. An electronic scale was positioned at the bottom of  
140 the stove to record the variation of fuel quality. Flue gases were drawn with a  
141 sampling gun (1.5 m higher than the flame) and then diluted ~30 times with a dilution  
142 system (TH-150, Wuhan Tianhong Ltd., China). The equipment settings can be  
143 referred to our previous studies (Yan et al., 2020, 2022). The diluted gases were  
144 collected into a 4 L Tedlar bag at a flow rate of  $150 \text{ mL min}^{-1}$ . The specific sampling  
145 systems can be seen in Figure S1. Each sampling practice covered a whole fuel-  
146 burning period. A total of 52 sets of samples were obtained.

147 For coal-fired power plants, 6 L summa cans were used to collect the flue gas  
148 after diluted. Each sampling time lasted for about 23 hours. The power plant has  
149 adopted ultra-low emission pollutant control measures, including wet desulfurization,



150 electric dust precipitation, and denitrification. Detailed information on the plant and  
151 field sampling settings can be found in our former research (Zeng et al., 2021).

## 152 **2.2 CFC-11 analysis, quality assurance and quality control**

153 CFC-11 was analyzed by a gas chromatography/mass spectrometry (GC-MS,  
154 Agilent 7820A/5977E). Samples were pretreated through a cold trap pre-concentrator  
155 before into the BD-624 chromatographic columns ( $60\text{ m} \times 0.25\text{ mm} \times 1.4\text{ }\mu\text{m}$ ). 300  
156 mL gases were extracted from the Tedlar bags or summa cans into a cold trap to  
157 remove water and  $\text{CO}_2$ . Then, the concentrated gases were sent to the gas  
158 chromatography with helium gas as the carrier gas. The gases passed through the  
159 chromatography column were divided into two sections, one for a FID detector and  
160 another one for a MS detector. The chromatographic column temperature increased  
161 from  $35\text{ }^\circ\text{C}$  to  $180\text{ }^\circ\text{C}$ , at a rate of  $6\text{ }^\circ\text{C min}^{-1}$ . The temperature for both the FID and  
162 MS detectors was  $200\text{ }^\circ\text{C}$ . The EI ionization mode of mass spectrum was adopted. The  
163 electron energy was  $70\text{ eV}$ . An internal standard method was used to calculate the  
164 concentration. Four internal standard substances including bromochloromethane, 1,4-  
165 difluorobenzene, chlorobenzene, and 4-bromofluorobenzene are used. CFC-11 was  
166 determined with a Mass Selective Detector (MSD) by the target ion at  $m/z\ 103/101$ ,  
167 and this method was widely used in previous research (Huang et al., 2021; Jin et al.,  
168 2025; Zhang et al., 2014). GC-MS was also used in other research for CFC-11  
169 observation (Park et al., 2021)

170 For quality control and quality assurance, tedlar bags were not reused in this  
171 study. A system blank test was conducted, after every 10 samples were analyzed and  
172 after the samples were analyzed at high concentrations. The calibration curves were  
173 updated monthly. A parallel sample was analyzed for every 10 samples or each batch  
174 (less than 10 samples), to ensure that the relative deviations of the targets were less  
175 than or equal to 30%. If the relative deviations exceeded 30%, then the sample was re-  
176 analyzed. Before each sample analysis, the air and water, the relative abundance of  
177 water, nitrogen, and oxygen should be less than 10%, otherwise the leakage of the



instrument system should be checked. The detection limit of CFC-11 was  $0.15 \mu\text{g m}^{-3}$ .

The concentration of CFC-11 in the blank sample of the instrument is 0.

### 2.3 Calculation method of CFC-11 emission

The EFs of CFC-11 from domestic coal combustion were calculated as follows:

$$EF_i = \frac{(c_i \times \frac{v}{v_1} \times n - c_0) \times v_1 \times t \times 10^{-6}}{M_i} \quad (1)$$

Where  $i$  stood for the fuel type;  $EF_i$  was the CFC-11 emission factor for combustion of fuel  $i$ ,  $\text{mg kg}^{-1}$ ;  $c_i$  was the mass concentration of CFC-11 in the sampling port after the combustion of fuel  $i$ ,  $\mu\text{g m}^{-3}$ ;  $v$  indicated the flow rate of flue gas,  $\text{L min}^{-1}$ ;  $v_1$  indicated the sampling flow rate,  $\text{L min}^{-1}$ ;  $n$  stood for dilution ratio;  $c_0$  was the mass concentration of CFC-11 in the atmospheric environment, in this study was  $0.6 \mu\text{g m}^{-3}$ ;  $t$  was the sampling time, min;  $M_i$  was the weight of fuel  $i$  burned, kg. The average mass concentration of CFC-11 from domestic coal combustion was  $93.9 \pm 90.4 \mu\text{g m}^{-3}$ , which was 150.7 times that of the ambient concentration, which indicated that the impact of ambient CFC-11 concentrations on its emission from coal combustion sources can be ignored.

The EFs of CFC-11 from coal-fired power plants were calculated as follows:

$$m_i = c_i \times v_1 \times t \times 10^{-6} \quad (2)$$

$$EF_{ij} = \frac{v \times m_i \times r_j^2 \times n}{v_1 \times M_i \times r^2} \quad (3)$$

Where  $i$  stood for the fuel type;  $m_i$  was the emission amount of CFC-11 released from the combustion of fuel  $i$ , mg;  $c_i$  was the mass concentration of CFC-11 from stack, which ignored the CFC-11 ambient concentration,  $\mu\text{g m}^{-3}$ ;  $v_1$  indicated the sampling flow rate,  $\text{L min}^{-1}$ ;  $t$  was the sampling time, min;  $EF_{ij}$  was the CFC-11 emission factor emitted by the combustion of coal  $i$  from power plant  $j$ ,  $\text{mg kg}^{-1}$ ;  $r_j$  was the semidiameter of the stack at the sampling point, m;  $r$  was the semidiameter of the sampling nozzle, m;  $n$  stood for dilution ratio;  $v$  indicated the flow rate of flue gas,  $\text{L min}^{-1}$ ;  $M_i$  was the weight of coal  $i$  burned, kg.

The CFC-11 emission amounts were calculated by multiplying its EFs (Table S2) with corresponding coal consumption amounts each year in China. The coal





consumption amounts for each province of China from 2000~2021 were obtained from the China Energy Statistical Yearbook, and there were no data for Hong Kong, Macao, Taiwan, and Xizang (China energy statistical yearbook). The coal consumption amounts from 2022~2060 were calculated according to the decrease rate in references (Wu et al., 2024; Energy Foundation, 2024). The spatial distribution of CFC-11 from domestic coal combustion was allocated according to the 2000~2018 land use data with 30 m\*30 m and 2000~2021 population distribution data with 1 km\*1 km (WorldPop and Center for International Earth Science Information Network) (Gong et al., 2019, 2020). The land use data for 2019~2021 used the data in 2018. The Point of Interest (POI) data of industrial were obtained to allocate the CFC-11 emission from coal-fired power plants into each plant (Figure S2). The specific calculation and allocation method could be found in our former studies (Cheng et al., 2022; Wu et al., 2021).

The CO<sub>2</sub>-equivalent (CO<sub>2</sub>-eq) emissions were calculated by multiplying the CFC-11 emission amounts with its global warming potential (GWP) value of 7090 (Burkholder et al., 2022).

## 2.4 WRF-FLEXPART modeling

Previous studies identified Shandong and Hebei provinces as the dominant source regions for CFC-11 detected on islands near Korea and Japan (Park et al., 2021). Here, we tried to explore the influence of CFC-11 emissions from coal combustion in the two provinces on its ambient levels. FLEXPART was usually employed for inverse estimating CFC-11 emissions by former researchers (An et al., 2012; Park et al., 2021; Rigby et al., 2019). Here, January was heating period with higher coal combustion, and the year 2016 had higher CFC-11 emissions (Montzka et al., 2018), January 2016 was selected as the simulated period. The meteorological input data were obtained and downloaded from National Centers for Environmental Prediction (NCEP) Final Analysis (FNL; <https://rda.ucar.edu/>), which provided the lateral boundary conditions and initial meteorological fields for the simulation. The



234 FNL data had a horizontal resolution of  $1^\circ \times 1^\circ$  and a temporal interval of 6 hours. The  
 235 simulation domain encompassed the East Asian region (within the boundary of  
 236  $20^\circ\sim 47^\circ\text{N}$  and  $110^\circ\sim 140^\circ\text{E}$ ). Hebei and Shandong were identified as the primary CFC-  
 237 11 release areas. The simulation period was set for January 2016 (similar to the  
 238 monitoring period in former studies) (Park et al., 2021), utilizing the forward  
 239 modeling approach for analysis. Air parcels were released from the gridded emission  
 240 areas over Hebei and Shandong provinces at altitudes from the surface up to 100 m,  
 241 reflecting the near-ground emissions from coal combustion.

### 242 3. Results and discussion

#### 243 3.1 CFC-11 EFs for coal combustion and comparison with other sources

244 The EFs of CFC-11 from chunk coal and honeycomb briquette combustion  
 245 varied from  $0.3\sim 12.7\text{ mg kg}^{-1}$  ( $3.6\pm 2.9\text{ mg kg}^{-1}$ ) and  $0.6\sim 4.2\text{ mg kg}^{-1}$  ( $3.2\pm 0.7\text{ mg}$   
 246  $\text{kg}^{-1}$ ), respectively (Figure 1). These values were 144 and 128 times higher than the  
 247 EF for coal-fired power plant ( $0.025\text{ mg kg}^{-1}$ ). The honeycomb briquette had higher  
 248 combustion efficiency than chunk coal, which may reduce the release of chloride and  
 249 formation of CFC-11 (Li et al., 2016). The much lower EFs for coal-fired power plant  
 250 could be related to the high combustion temperature and series of flue gas treatment  
 251 measures (Yan et al., 2016). CFC-11 includes chloride (Cl) and fluoride (F), the  
 252 formation of CFC-11 needs the participation of Cl and F. F and Cl were widely  
 253 distributed in Chinese coal. Former studies indicated that F content was  $20\sim 300$   
 254  $\text{mg/kg}$  from coals in the North China Plate and Northwest China, lower than the  
 255 Southwest China ( $50\sim 3000\text{ mg/kg}$ ) (Luo et al., 2004). The chlorine content of  
 256 bituminous coal was  $252.5\text{ mg kg}^{-1}$  in China (Jin et al., 2025). The formation and  
 257 emission mechanisms of CFC-11 during coal combustion remained unclear. There  
 258 was only one old literature reported that CFC-11 could be detected from the  
 259 combustion of all tested 23 types of coal, and the release of CFC-11 peaked at a  
 260 combustion temperature of  $400^\circ\text{C}$  (Li et al., 2004). Coal combustion could emit  
 261 halogenated organic compounds, such as methyl chloride ( $\text{CH}_3\text{Cl}$ ) and chloroform



(CH<sub>2</sub>Cl<sub>2</sub>) (Liu et al., 2024). Recent research presented the possible formation route of CFC-11 from above halogenated organic compounds in the iron and steel industry, based on the traditional liquid-phase fluorination method (Liu et al., 2024). This exploratory study primarily deduced that the formation conditions of CFC-11 in coal combustion were similar to the industrial synthesis conditions of CFC-11. The transformation pathways of solid fluoride in coal to CFC-11 and influencing parameters were still a puzzle. The mechanisms driving the formation and release of CFC-11, as well as the dominant influencing factors, remain unexplored and warrant further investigation.

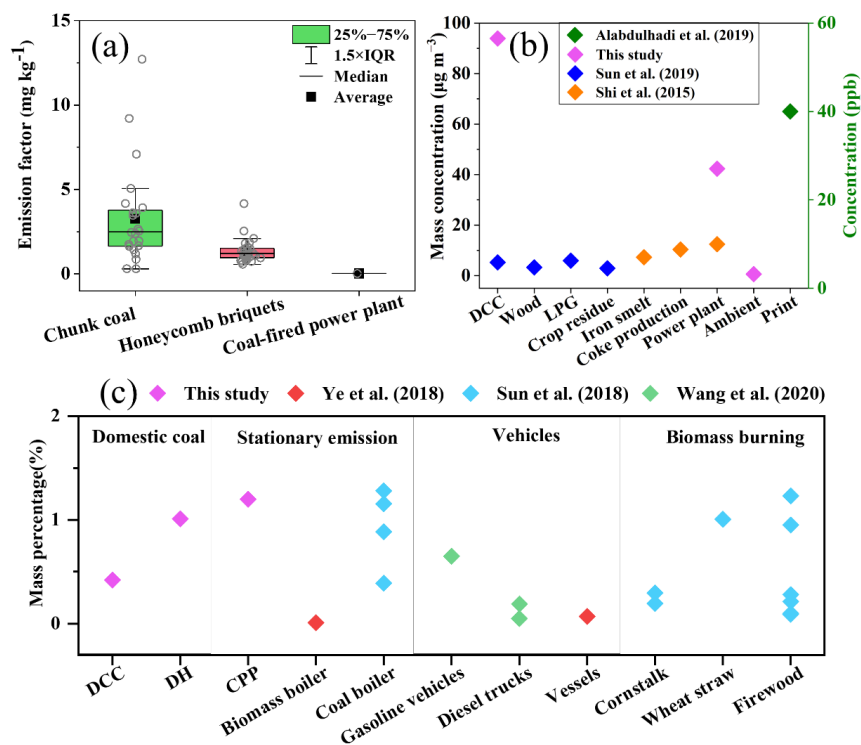


**Figure 1.** Comparison of CFC-11 emission from coal combustion and other sources for its emission factor (a), mass concentration (b), and mass percentage (c) in total VOCs. The VOCs included 102, 61, 107, 101, 98, and 102 species in this study, Sun et al. (2019), Shi et al. (2015), Ye et al. (2018), Sun et al. (2018), and Wang et al. (2020), respectively. DCC means domestic chunk coal, DH means domestic honeycomb, and CPP means coal-fired power plant.



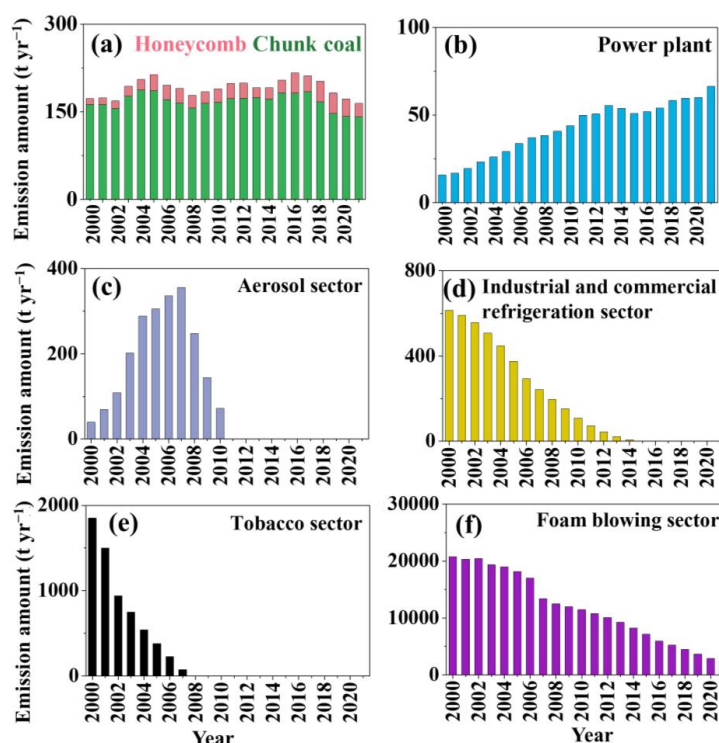
277 Previous studies have reported the emission of CFC-11 from other anthropogenic  
 278 sources (Gong et al., 2019; Sun et al., 2019). Domestic anthracite coal combustion  
 279 ( $5.2 \mu\text{g m}^{-3}$ ) (Sun et al., 2019), coating ( $44.5 \mu\text{g m}^{-3}$  and  $91.0 \mu\text{g m}^{-3}$ ), and printing  
 280 ( $40 \text{ ppb}$  and  $10.9 \mu\text{g m}^{-3}$ ) all emitted CFC-11 (Alabdulhadi et al., 2019; Shen et al.,  
 281 2018). Figure 1b presented the CFC-11 mass concentration for reported combustion  
 282 sources in the literature, coal-fired power plants ( $42.3 \mu\text{g m}^{-3}$ ), iron smelting ( $7.3 \mu\text{g m}^{-3}$ )  
 283 ( $10.3 \mu\text{g m}^{-3}$ ), and coal-fired power plants ( $12.5 \mu\text{g m}^{-3}$ ) (Shi et  
 284 al., 2015) all were the CFC-11 emission sources. The CFC-11 accounted for 0.4%,  
 285 1.0%, and 1.2% of the total volatile organic compounds (VOCs) detected from the  
 286 combustion of chunk coal, honeycomb briquette, and coal-fired power plant in this  
 287 study, respectively. These proportions were higher than those for stationary  
 288 combustion of biomass (0.01%) (Ye, 2018), heavy-duty diesel trucks (0.05% or 0.2%)  
 289 (Wang et al., 2020), vessels (0.07%) (Ye, 2018) and corn stover burning (0.3% or  
 290 0.2%) reported in the literature (Figure 1c) (Sun et al., 2018). The CFC-11 mass  
 291 percentages for VOCs emitted from stationary coal combustion and firewood burning  
 292 were 0.4%~1.3% and 0.1%~1.2% (Sun et al., 2018), similar to this study. Ground  
 293 measurement campaigns also recorded high CFC-11 levels from specific events, such  
 294 as 626 ppt and 658 ppt for garbage burning and a landfill fire near Mecca,  
 295 respectively (Simpson et al., 2022). Although combustion-related CFC-11 emissions  
 296 were influenced by combustion conditions, these findings provided evidence for the  
 297 contribution of coal combustion and other combustion sources to overall CFC-11  
 298 emissions.

### 299 3.2 Spatial-temporal distribution of CFC-11 from coal combustion in China

300 The annual CFC-11 emissions from coal combustion in China during 2000~2021  
 301 exhibited fluctuations and an overall upward trend, peaking at  $268.7 \text{ t yr}^{-1}$  in 2016  
 302 (Figures 2a–2b). CFC-11 emissions increased after 2012, consistent with previous  
 303 studies that reported rising CFC-11 concentrations in ambient air (Adcock et al., 2020;  
 304 Montzka et al., 2018; Rigby et al., 2019). Approximately 40%~60% of the global



305 increase in CFC concentration was attributed to China, particularly Shandong and  
 306 Hebei provinces (Adcock et al., 2020; Montzka et al., 2018; Rigby et al., 2019). This  
 307 study found marked increases in CFC-11 emissions from Hebei (14.3 t yr<sup>-1</sup>) and  
 308 Shandong (11.0 t yr<sup>-1</sup>) in 2013, which were 2.2 and 1.4 times the respective emission  
 309 amounts in 2012 (Figure 3). The emission of CFC-11 emissions from coal combustion  
 310 in China fluctuated during 2001~2021, averaging 233.5 t yr<sup>-1</sup>. The contribution of  
 311 coal combustion to CFC-11 emissions on a global scale needs further research.



312  
 313 **Figure 2.** Annual CFC-11 emission from domestic coal combustion (a), coal-fired power plant (b),  
 314 aerosol sectors (c), industrial and commercial refrigeration sector (d), tobacco sector (e), and foam  
 315 blowing sector (f) in China. The data for (a) and (b) were calculated in this study. The data for  
 316 (c)~(f) referred to Fang et al. (2018).

317 Although the contribution of domestic chunk coal combustion to CFC-11 annual  
 318 emissions decreased from 2000 to 2021, it was still the dominant contributor,  
 319 accounting for 60.9%~86.4% of CFC-11 emissions of domestic coal combustion in



China (Figure 3). By 2021, the cumulative CFC-11 emissions from coal combustion  
 reached 5135.7 t in China (Figure S3), with domestic coal combustion contributing  
 4200.0 t and coal-fired power plant contributing 935.7 t. With the transformation of  
 China's energy structure, the proportion of CFC-11 emissions from coal-fired power  
 plants in total CFC-11 emissions from coal combustion increased from 7.9% in 2000  
 to 18.2% in 2021.

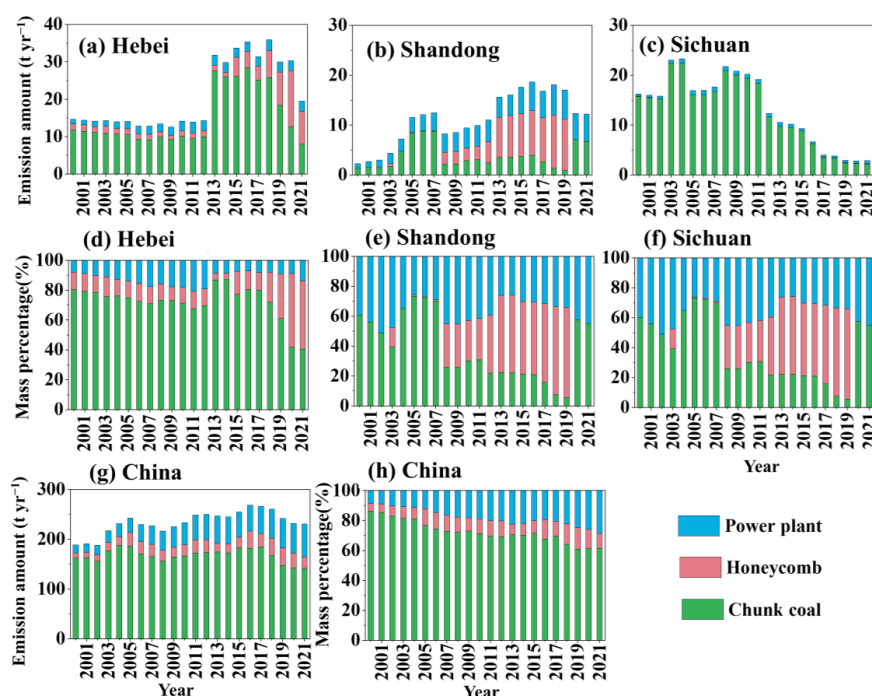


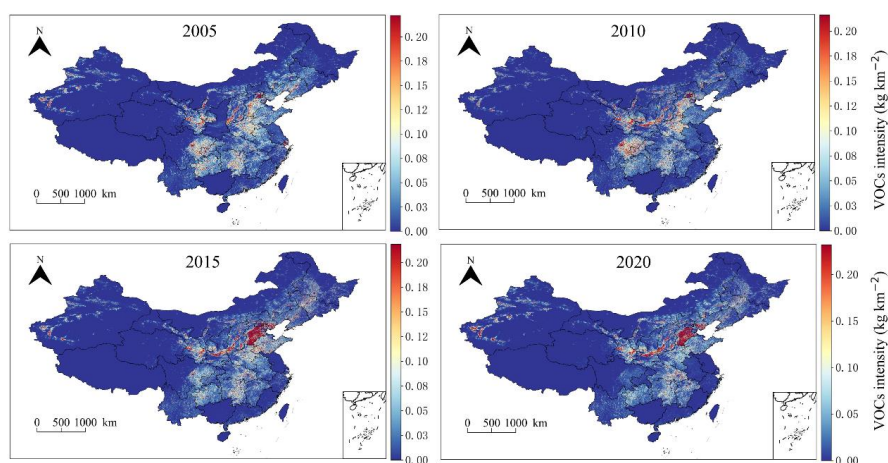
**Figure 3.** The CFC-11 emissions (a~c) and mass percentages (d~f) from power plant, domestic  
 chunk coal, and honeycomb combustion in Hebei, Shandong, and Sichuan provinces.

Previous studies have constructed CFC-11 emission inventories for its PAU  
 processes and formed a PAU emission bank (Fang et al., 2018; Wan et al., 2009),  
 which mainly included the sectors of aerosol, industrial and commercial refrigeration,  
 tobacco, and foam-blowing in China as Figures 2c–2f shown. The CFC-11 emission  
 amounts from coal combustion were comparable with those from aerosol sector and  
 industrial and commercial refrigeration. The CFC-11 emissions from aerosol sector  
 and tobacco sector disappeared after 2010 and 2007 as the Montreal Protocol,



336 respectively. After 2015, the foam-blowing sector became the sole contributor to  
 337 CFC-11 emissions among these sectors, with its emission declining to  $7155.9 \text{ t yr}^{-1}$ . If  
 338 all other CFC-11 emissions from PAU sources were gradually getting to zero, while  
 339 the CFC-11 emissions from coal combustion persisted, the influence of CFC-11  
 340 emissions from coal combustion should be considered at that time, especially when  
 341 the CFC-11 emissions from PAU were cleared to zero.

342 Figure S4 presents the CFC-11 emissions from coal combustion in different  
 343 provinces in China during 2000~2021. Provinces in heating areas exhibited high  
 344 CFC-11 emissions throughout the study period, they were in the north of China. Such  
 345 as Inner Mongolia, Hebei, Henan, Xinjiang, Shandong, and Shanxi, the CFC-11  
 346 emissions in 2021 were 36.1 t, 19.5 t, 10.0 t, 21.2 t, 12.2 t, and 15.2 t respectively.  
 347 Figure 4 shows the CFC-11 emission intensity of CFC-11 from domestic coal  
 348 combustion. High-emission areas were consistently concentrated in the North China  
 349 Plain, including Hebei, Shandong, and Henan, where residential coal consumption has  
 350 historically been significant. Over time, these high-emission zones became more  
 351 pronounced, particularly after 2013.



352  
 353 **Figure 4.** CFC-11 emission intensity of CFC-11 from domestic coal combustion in 2005, 2010,  
 354 2015, and 2020.



### 3.3 Comparison with CFC-11 emission obtained from CFC/CO ratios

In this study, the slope of CFC-11 and CO from coal combustion was 0.447 (Figure 5), higher than 0.039~0.087 in the atmosphere (Huang et al., 2021). CFC-11 emission inventory from coal combustion was obtained according to the CO emission inventory from coal combustion and CFC-11/CO ratio. Figure 5b presents the CFC-11 emission from coal combustion using CO tracer method and bottom-up method. The CFC-11 emission through CO tracer method was 7872~60466 kt yr<sup>-1</sup>, much higher than the emission using bottom-up method (7.9~60.8 t yr<sup>-1</sup>). Although the ratio method using CO as a tracer was commonly applied in estimations, it might lead to an overestimation of CFC-11 emissions. Since CO had many emission sources, if the ratio was calculated using CFC-11/CO in the atmospheric concentration, then CFC-11 was also assumed to come from these emission sources. From previous research, CFC-11 emission from combustion sources, including industrial processes, vehicle emissions, garbage burning, LPG, and biomass burning, had long been overlooked (Shen et al., 2018; Wu & Xie, 2017; Zhang et al., 2020). However, the growing significance of these emissions highlighted the need for a more comprehensive evaluation of all potential sources for CFC-11, including above combustion sources and non-combustion sources like fuel oil storage, oil transportation, and printing facilities (Alabdulhadi et al., 2019b).

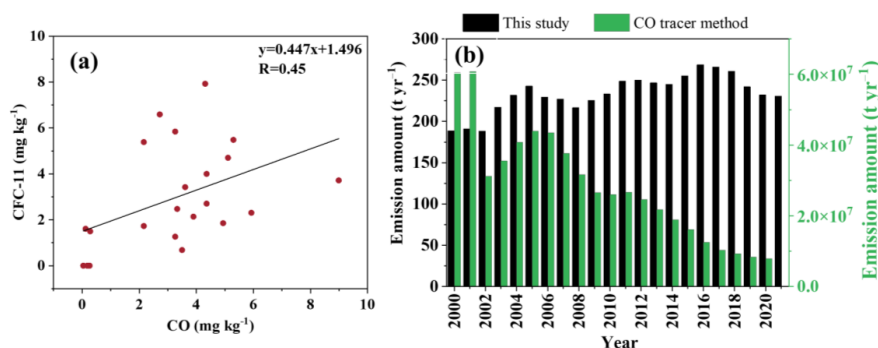


**Figure 5.** Interspecies correlations of CFC-11 with CO from coal combustion,  $R$ =Pearson's  $r$  (a), and comparison of CFC-11 emissions from coal combustion between this study and the CO tracer





method. The emission inventory of CO for coal combustion was referred to previous studies (b) (Liu et al., 2015; Peng et al., 2019; Tong et al., 2018).

### 3.4 Increasing importance of coal combustion in CFC-11 emission

A lot of research calculated the CFC-11 emissions in China and even globally based on ambient monitoring data (Table S3), the CFC-11 emissions from coal combustion were smaller than all CFC-11 emissions in China. The proportion of CFC-11 emissions from coal combustion relative to its bank emissions increased year by year from 2000 (Figure 6a). The annual CFC-11 emissions from coal combustion in China from 2000 to 2021 varied from 188.5~268.7 t yr<sup>-1</sup>, accounting for 1.5%~2.1% of the global increase in CFC-11 emission of 13±5 kt yr<sup>-1</sup> reported in the literature (Montzka et al., 2018). In 2000, the CFC-11 emission from coal combustion was 188.5 t yr<sup>-1</sup>, only accounting for 0.8% of PAU emissions in China. By 2021, however, CFC-11 emissions from coal combustion had risen to 9.8% of PAU emissions according to Figure 6a. After 2025, the CFC-11 emissions from PAU in China was 0, but the CFC-11 from coal combustion still existed as seen in Figure S5, subsequent controls should give greater consideration to coal combustion because of its widespread sources (Jin et al., 2025).

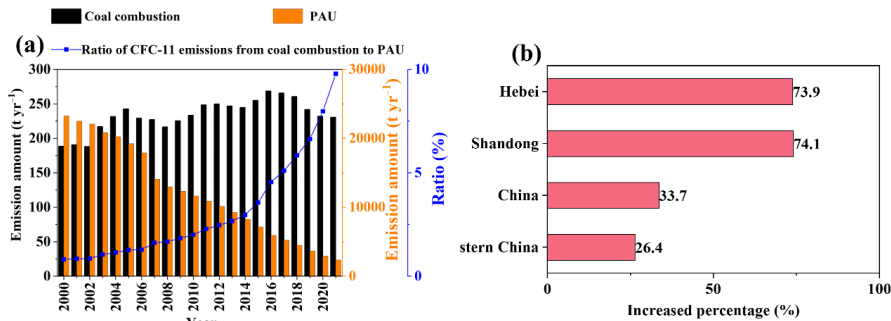


**Figure 6.** (a) Comparison of CFC-11 emission amounts from coal combustion (including coal consumed in domestic use and power plant) with CFC-11 emission from production and use (PAU) including aerosol sectors, tobacco sector, foam blowing sector, and industrial and commercial refrigeration sector in China (Fang et al., 2018). (b) The increased percentages for CFC-11 in this study in 2014~2017 compared to 2011~2012.



400 CFC-11 emissions from coal combustion increased sharply in 2013 as seen in  
401 Figure 2. From 2014 to 2017, CFC-11 emissions from coal combustion in China,  
402 Shandong Province, and Hebei Province increased compared to their corresponding  
403 emissions in the 2011~2012 period, the increasing ratios were 33.7%, 74.1%, and  
404 73.9%, respectively (Figure 6b). Previous studies indicated that the concentration of  
405 CFC-11 in the northern hemisphere's atmosphere in 1995 was approximately 267 ppt  
406 (Montzka et al., 2018). In 2060, the concentration of CFC-11 is 136.7 ppt, and in 2100,  
407 the concentration of CFC-11 still has 69.5 ppt (Daniel et al., 2022). Considering the  
408 lifetime of CFC-11 is about 52 years (Burkholder et al., 2022), we inferred that coal  
409 combustion might slightly contribute to the 136.7 ppt and 69.5 ppt of CFC-11.

### 410 3.5 Additional climate benefits of clean heating and coal-to-electricity policies

411 As the clean coal and heating policies were implemented, the coal consumption  
412 structures differed in southern (taking Sichuan as an example) and northern provinces  
413 (Hebei and Shandong) and changed quickly, which led to a clear variation of CFC-11  
414 emission from coal combustion (Figure 3). The CFC-11 emission from honeycomb  
415 briquette combustion increased for Hebei and Shandong Province after 2013 when the  
416 Action Plan for Air Pollution Prevention and Control in China was released (Geng et  
417 al., 2024). In Sichuan province, CFC-11 emissions from chunk coal combustion  
418 decreased significantly, especially after 2013. By 2020, no CFC-11 emissions from  
419 honeycomb briquette combustion were detected in Shandong and Sichuan Province.

420 With the replacement of chunk coal with honeycomb briquette and coal-to-  
421 electricity policy, the emission of CFC-11 from chunk coal combustion gradually  
422 decreased after 2016 for China (Figure S5). Domestic coal combustion was projected  
423 to cease entirely by 2030 (Energy Foundation, 2024), and CFC-11 emissions from  
424 coal-fired power plant decreased gradually to zero in 2060 to realize carbon neutrality  
425 (Figure S5) (Wu et al., 2024). From 2000 to 2060, the cumulative CFC-11 emissions  
426 from coal combustion in China will be 7115.0 t. Even though the coal consumption  
427 structure had changed (Shen et al., 2022), coal combustion remained a stable emission



428 source of CFC-11. Its accumulated emission amounts were similar to the historical  
 429 (2000–2060) CFC-11 emissions from tobacco sector (6263 t), and higher than that of  
 430 aerosol sector (4233 t) and industrial and commercial refrigeration (2169 t).

431 Figure 7 illustrates the CO<sub>2</sub>-eq emissions in China from coal combustion  
 432 between 2000 to 2021. In 2021, the CO<sub>2</sub>-eq emissions reached  $1.7 \times 10^6$  t yr<sup>-1</sup>,  
 433 accounting for 0.02% of total anthropogenic CO<sub>2</sub> emissions in China and 0.2% of CO<sub>2</sub>  
 434 emissions from cement from Global Carbon Atlas. This value accounted for 0.03% of  
 435 China's forest carbon sink ( $6.6 \times 10^9$  t CO<sub>2</sub>) (Liu et al., 2015; Pan et al., 2011). These  
 436 findings highlighted the need to reassess the role of CFC-11 from combustion  
 437 emissions in global warming potential. From Figure 7b, the contribution of chunk coal  
 438 combustion to CO<sub>2</sub>-eq emissions decreased from 89.3% in 2000 to 63.3% in 2021 and  
 439 would decrease to 0 after 2030. The replacement of chunk coal with honeycomb  
 440 briquette resulted in a decrease of 25.2% in chunk coal usage and 8.9% in honeycomb  
 441 usage (China Energy Statistical Yearbook). During 2000–2021, if all chunk coal was  
 442 replaced by honeycomb briquette, CFC-11 and CO<sub>2</sub>-eq emissions would be reduced  
 443 by 10.6–16.0 t yr<sup>-1</sup> and  $7.5 \times 10^4 \sim 1.1 \times 10^5$  t yr<sup>-1</sup>, respectively (Figures S6 and 7c).  
 444 This study verified the necessity of energy mix adjustment and the use of clean energy,  
 445 from the aspect of co-prevention and control of multi-pollutants and the win-win in  
 446 climate-environmental benefits (Shen et al., 2019; Shen et al., 2021; Tao et al., 2021).  
 447 Although the decreased CFC-11 and CO<sub>2</sub>-eq emissions were small, their impacts on  
 448 the ozone layer and climate change should not be underestimated because of the  
 449 extensive and universal sources of CFC-11 emissions (Jin et al., 2025).

450 In contrast, the contribution of coal-fired power plant to CO<sub>2</sub>-eq emissions  
 451 increased from 6.8% in 2000 to 28.0% in 2021 and was expected to rise to 100% after  
 452 2030. The coal-to-electricity strategy implemented in China increased the coal  
 453 consumption in power plant (Wang et al., 2020), significantly reducing CFC-11  
 454 emissions from domestic coal combustion by 170.1–252.0 t yr<sup>-1</sup> and reducing CO<sub>2</sub>-eq  
 455 emissions by  $1.2 \times 10^6 \sim 1.8 \times 10^6$  t yr<sup>-1</sup> during 2000–2021 (Figures S6 and 5d). It



indicates that transitioning to cleaner coal alternatives can not only improve the air quality in the North China Plain (Fang et al., 2019), but also yield unexpected significant climate benefits by reducing CFC-11 and CO<sub>2</sub>-eq emissions. However, CFC-11 has a very large and uncertain indirect radiative cooling effect due to its depletion of Ozone, resulting in an indirect GWP of -4390 (Daniel et al., 2022). CO<sub>2</sub>-eq emission in this study was calculated using direct GWP, relying solely on the direct GWP might overestimate its climate impact. Therefore, a more comprehensive approach was essential for accurately assessing the full climate impact of CFC-11 and informing effective mitigation strategies.

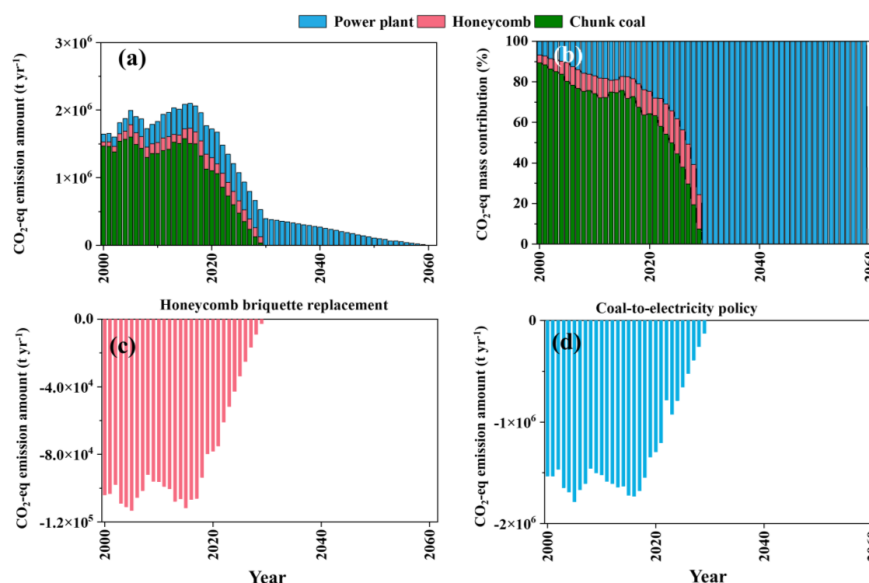


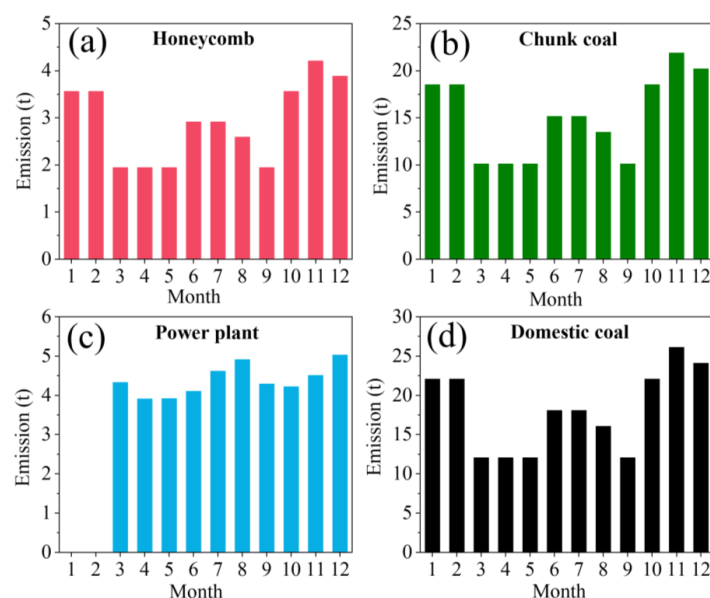
**Figure 7.** CO<sub>2</sub>-eq emissions for CFC-11 emitted from coal combustion in China in this study (a) and (b). The changes of CO<sub>2</sub>-eq emissions from CFC-11, if coal was replaced by honeycomb (c) and if domestic coal was replaced by electricity produced in coal-fired power plant (d).

### 3.6 The influence of CFC-11 from coal combustion on ambient concentration

Former researchers indicated that additional emission of CFC-11 was found in 2016 (Montzka et al., 2018; Rigby et al., 2019), monthly CFC-11 emission is presented in Figure 8. The monthly CFC-11 emissions from domestic coal combustion were allocated according to Wu et al. (2021), from coal-fired power plant were



474 allocated according to the power generation volume from National Bureau of  
 475 Statistics of China (<https://www.stats.gov.cn/>). The higher CFC-11 emissions from  
 476 domestic coal combustion were in cold months, January (22.1 t), February (22.1 t),  
 477 October (22.1 t), November (26.1 t), and December (24.1 t). The higher CFC-11  
 478 emissions from coal-fired power plant were in August (4.9 t) and December (5.0 t).



479  
 480 **Figure 8.** Monthly CFC-11 emissions from domestic honeycomb briquette combustion (a),  
 481 domestic chunk coal combustion (b), coal-fired power plant (c), and domestic coal combustion (d)  
 482 in 2016. The CFC-11 emissions from coal-fired power plant in January and February didn't have  
 483 specific data.

484 Shandong and Hebei Province were regarded as the hot source regions of CFC-  
 485 11 (Montzka et al., 2018; Rigby et al., 2019), from Figure 9a, Hebei and Shandong  
 486 provinces held high emission intensities of CFC-11 from coal combustion, with  
 487 average emission intensities of 0.23 and 0.03 kg km<sup>-2</sup>, respectively. We also found that  
 488 the CFC-11 emission from coal combustion in Hebei and Shandong provinces peaked  
 489 in 2016 (Figures 9b–9c). They increased by 11.2% and 19.7%, compared with those  
 490 of 2013, then decreased by 15.2% and 8.6% in 2019, respectively. Based on the WRF-



491 FLEXPART modeling, we found that the CFC-11 emissions from coal combustion in  
492 Shandong and Hebei provinces could impact South Korean areas (Figures 9d–9e).  
493 After being emitted from coal combustion in the two provinces, CFC-11 could  
494 contribute to the monitored atmospheric concentrations in January as 254~1062 ppt  
495 within 410 km surrounding the emission source regions, higher than the observed  
496 value of  $249 \pm 13$  ppt at Mount Tai in winter 2017 to spring 2018 (Huang et al., 2021),  
497 this distance might not influence the monitoring station outside China. Specifically,  
498 CFC-11 emissions from coal combustion in Hebei were simulated to contribute 51.8  
499 ppt of the ambient CFC-11 at the Gosan station in South Korea. Similarly, the  
500 contributions from Shandong were simulated as 17.6 ppt. At the Gosan station in  
501 South Korea, the measured CFC-11 concentration was 233.2 ppt in January 2021  
502 through the Advanced Global Atmospheric Gases Experiment (AGAGE, [https://www-  
503 air.larc.nasa.gov/missions/agage/](https://www-air.larc.nasa.gov/missions/agage/)). Our simulations suggested that CFC-11 emissions  
504 from coal combustion in Hebei and Shandong contributed approximately 51.8 ppt and  
505 17.6 ppt, respectively. They accounted for ~30% of the measured ambient value.

506 Although this suggested that regional coal combustion sources could slightly  
507 influence background monitoring data in coastal East Asia, the contribution remained  
508 much smaller than from global PAU-related emissions and must be interpreted  
509 cautiously. Notably, the results here also exhibited uncertainties or shortages. Firstly,  
510 the CFC-11 emission factors from chunk coal and honeycomb briquettes varied in a  
511 large range, with the ratios of maximum to minimum values as 42 and 7 times, and  
512 relative standard deviations of 61% and 81%, respectively. Secondly, the quick  
513 variation of domestic coal consumption amount and structure had not been reflected  
514 in the statistical yearbooks. The uncertainty of CFC-11 emission inventory from coal  
515 combustion in this study was  $\pm 39.1\%$  through 100000 Monte Carlo simulations.

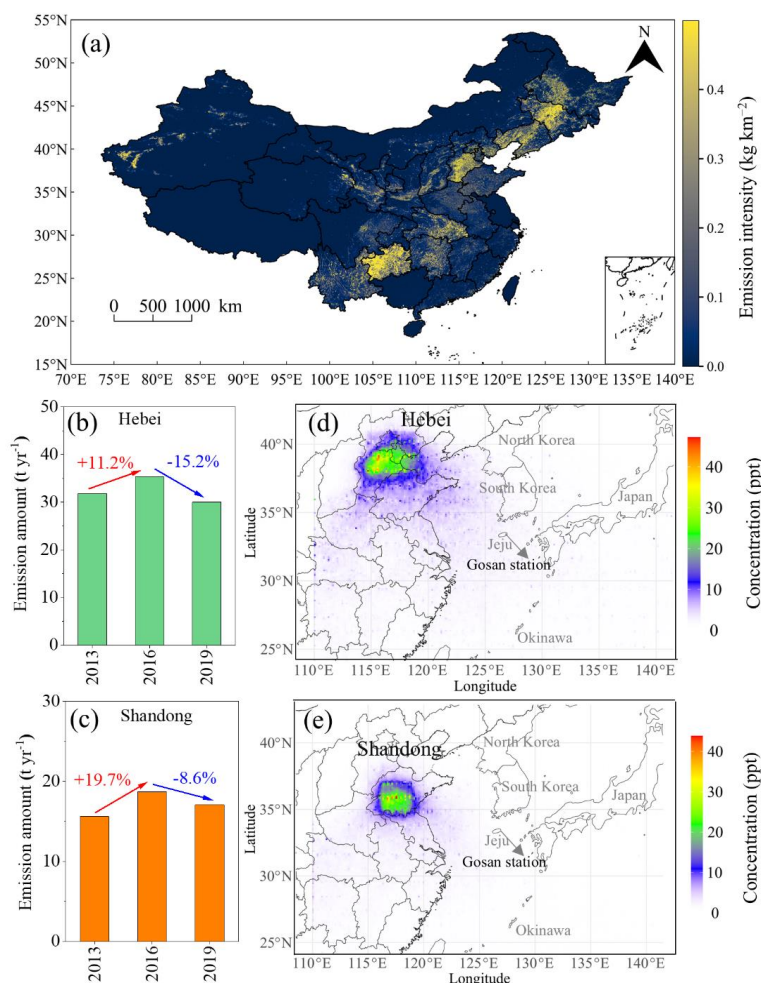


**Figure 9.** The emission intensity ( $\text{kg km}^{-2}$ ) of CFC-11 from coal combustion in 2016 (a), and the changes of CFC-11 from coal combustion in 2013, 2016, and 2019 in Hebei province (b) and Shandong province (c) in China. The distribution of simulated CFC-11 mass concentration contributed by coal combustion in January 2016 from Hebei (d) and Shandong (e) provinces with WRF-FLEXPART.

#### 4. Data availability

The dataset presented is available at <https://doi.org/10.6084/m9.figshare.28523063> (Niu et al., 2025). The activity data of coal combustion were from the China Energy Statistical Yearbook. Land use data was from <https://data-starcloud.pcl.ac.cn/> (Gong et al., 2019, 2020). Population



distribution data were from <https://hub.worldpop.org/doi/10.5258/SOTON/WP00674> (WorldPop and Center for International Earth Science Information Network). The POI data of industrial were obtained from <https://lbs.amap.com/>. The CO emissions from coal combustion in China were from <http://meicmodel.org.cn/#firstPage> (Multiresolution Emission Inventory for China). The meteorological input data were obtained and downloaded from <https://rda.ucar.edu/> (National Centers for Environmental Prediction Final Analysis).

## 5. Conclusions

There is currently no quantitative research on CFC-11 emissions from coal combustion. This study addresses that gap by estimating CFC-11 emissions in China from 2000 to 2021, based on coal consumption data and experimentally determined emission factors. The measured CFC-11 EFs were 3.6, 3.2, and 0.025 mg kg<sup>-1</sup> for domestic chunk coal, honeycomb briquettes, and coal-fired power plants, respectively. During the study period, total CFC-11 emissions from coal combustion in China were estimated at 233.5 t yr<sup>-1</sup>. In Shandong and Hebei provinces, which have high levels of coal consumption, CFC-11 emissions increased by approximately 74% during 2014~2017 compared to 2011~2012. At the Gosan monitoring station near mainland China, emissions from Hebei and Shandong accounted for approximately 30% of the average CFC-11 concentration in January 2016. Notably, China's clean heating and coal-to-electricity policies also brought climate co-benefits, resulting in significant reductions of CO<sub>2</sub>-equivalent emissions by 2.2×10<sup>6</sup> tons and 3.4×10<sup>7</sup> tons, respectively. This study provides quantitative evidence of CFC-11 emissions from coal combustion, but the formation mechanisms of CFC-11 from coal combustion are unclear and need further investigation.

## Author contributions:

Zhenzhen Niu: Conceptualization, Experiments, Visualization, Writing; Shaofei Kong: Conceptualization, Methodology, Supervision, Writing-review & editing. Qin Yan, Yi





555 Cheng, Huang Zheng, and Jian Wu: Experiments. Yao Hu, Xujing Qin, Haoyu Dong,  
556 Weisi Jiang: Visualization. Yingying Yan, Wei Liu, Feng Ding, Yongqing Bai, and  
557 Shihua Qi: Supervision.

558 **Competing interests:**

559 The contact author has declared that none of the authors has any competing interests.

560 **Financial Support:**

561 This work was supported by the Key Technologies Research and Development  
562 Program (grant no. 2023YFC3709802), the Hubei Provincial Science Fund for  
563 Distinguished Young Scholars (grant no. 2022CFA040), and the National Natural  
564 Science Foundation of China (grant no. 42077202).



## 565 References

- 566 Adcock, K. E., Ashfold, M. J., Chou, C. C.-K., Gooch, L. J., Mohd Hanif, N., Laube,  
 567 J. C., et al. (2020). Investigation of East Asian emissions of CFC-11 using  
 568 atmospheric observations in Taiwan. *Environmental Science & Technology*, 54(7),  
 569 3814–3822. <https://doi.org/10.1021/acs.est.9b06433>
- 570 Alabdulhadi, A., Ramadan, A., Devey, P., Boggess, M., & Guest, M. (2019).  
 571 Inhalation exposure to volatile organic compounds in the printing industry.  
 572 *Journal of the Air & Waste Management Association*, 69(10), 1142–1169.  
 573 <https://doi.org/10.1080/10962247.2019.1629355>
- 574 An, X., Henne, S., Yao, B., Vollmer, M. K., Zhou, L., & Li, Y. (2012). Estimating  
 575 emissions of HCFC-22 and CFC-11 in China by atmospheric observations and  
 576 inverse modeling. *Science China Chemistry*, 55(10), 2233–2241.  
 577 <https://doi.org/10.1007/s11426-012-4624-8>
- 578 Burkholder, J. B., Hodnebrog, Ø., McDonald, B. C., Orkin, V., Papadimitriou, V. C.,  
 579 & Van Hoomissen, D. (2022). Summary of abundances, lifetimes, ODPs, REs,  
 580 GWPs, and GTPs. World Meteorological Organization (WMO), Geneva,  
 581 Switzerland. <https://csl.noaa.gov/assessments/ozone/2022/>
- 582 Cheng, Y., Kong, S., Yao, L., Zheng, H., Wu, J., Yan, Q., et al. (2022). Multiyear  
 583 emissions of carbonaceous aerosols from cooking, fireworks, sacrificial incense,  
 584 joss paper burning, and barbecue as well as their key driving forces in China.  
 585 *Earth System Science Data*, 14(10), 4757–4775. [https://doi.org/10.5194/essd-14-](https://doi.org/10.5194/essd-14-4757-2022)  
 586 4757-2022
- 587 Chiodo, G., & Polvani, L. M. (2022). New insights on the radiative impacts of ozone-  
 588 depleting substances. *Geophysical Research Letters*, 49(10), e2021GL096783.  
 589 <https://doi.org/10.1029/2021GL096783>
- 590 Daniel, J. S., Reimann, S., Ashford, P., Fleming, E. L., Hossaini, R., Lickley, M. J., et  
 591 al. (2022). 2022 Ozone Assessment, United Nations Environment Programme:  
 592 Nairobi, Kenya, 390–430. From chrome-



593 extension://efaidnbmnnnibpcajpcglclefindmkaj/https://csl.noaa.gov/assessments/  
 594 ozone/2022/downloads/Chapter7\_2022OzoneAssessment.pdf  
 595 Dhomse, S. S., Feng, W., Montzka, S. A., Hossaini, R., Keeble, J., Pyle, J. A., et al.  
 596 (2019). Delay in recovery of the Antarctic ozone hole from unexpected CFC-11  
 597 emissions. *Nature Communications*, 10(1), 5781. https://doi.org/10.1038/s41467-  
 598 019-13717-x  
 599 Fang, X., Ravishankara, A. R., Velders, G. J. M., Molina, M. J., Su, S., Zhang, J., et al.  
 600 (2018). Changes in emissions of ozone-depleting substances from China due to  
 601 implementation of the Montreal Protocol. *Environmental Science & Technology*,  
 602 52(19), 11359–11366. https://doi.org/10.1021/acs.est.8b01280  
 603 Fang, D., Chen, B., Hubacek, K., Ni, R., Chen, L., Feng, K., et al. (2019). Clean air  
 604 for some: unintended spillover effects of regional air pollution policies. *Science*  
 605 *Advances*, 5(8), eaav4707. https://doi.org/10.1126/sciadv.aav4707  
 606 Fleming, E. L., Newman, P. A., Liang, Q., & Daniel, J. S. (2020). The impact of  
 607 continuing CFC-11 emissions on stratospheric ozone. *Journal of Geophysical*  
 608 *Research: Atmospheres*, 125(3), e2019JD031849.  
 609 https://doi.org/10.1029/2019JD031849  
 610 Geng, G., Liu, Y., Liu, Y., Liu, S., Cheng, J., Yan, L., et al. (2024). Efficacy of China's  
 611 clean air actions to tackle PM<sub>2.5</sub> pollution between 2013 and 2020. *Nature*  
 612 *Geoscience*, 17, 987–994. https://doi.org/10.1038/s41561-024-01540-z  
 613 Global Carbon Atlas. Carbon Emissions. Available at:  
 614 https://globalcarbonatlas.org/emissions/carbon-emissions/ (accessed December  
 615 22, 2024).  
 616 Gong, P., Chen, B., Li, X., Liu, H., Wang, J., Bai, Y., et al. (2020). Mapping essential  
 617 urban land use categories in China (EULUCChina): Preliminary results for 2018,  
 618 *Science Bulletin*, 65, 182–187. https://doi.org/10.1016/j.scib.2019.12.007



- 619 Gong, P., Li, X., & Zhang, W. (2019). 40-Year (1978–2017) human settlement  
620 changes in China reflected by impervious surfaces from satellite remote sensing,  
621 *Science Bulletin*, 64(11), 756–763. <https://doi.org/10.1016/j.scib.2019.04.024>
- 622 Guo, H., Ding, A., Wang, T., Simpson, I. J., Blake, D. R., Barletta, B., et al. (2009).  
623 Source origins, modeled profiles, and apportionments of halogenated  
624 hydrocarbons in the greater Pearl River Delta region, Southern China. *Journal of*  
625 *Geophysical Research: Atmospheres*, 114(D11), 2008JD011448.  
626 <https://doi.org/10.1029/2008JD011448>
- 627 Huang, X., Zhang, Y., Xue, L., Tang, J., Song, W., Blake, D. R., & Wang, X. (2021).  
628 Constraining emission estimates of CFC-11 in Eastern China based on local  
629 observations at surface stations and Mount Tai. *Environmental Science &*  
630 *Technology Letters*, 8(11), 940–946. <https://doi.org/10.1021/acs.estlett.1c00539>
- 631 Jin, W., Yan, Y., Qiu, X., Peng, L., Li, Z., & Tang, Y. (2025). Characterizing full-phase  
632 chlorine species emissions from domestic coal combustion in China:  
633 Implications for significant impacts on air pollution and ozone-layer depletion.  
634 *Environmental Pollution*, 372, 126043.  
635 <https://doi.org/10.1016/j.envpol.2025.126043>
- 636 Kim, J., Li, S., Kim, K., Stohl, A., Mühle, J., Kim, S., et al. (2010). Regional  
637 atmospheric emissions determined from measurements at Jeju Island, Korea:  
638 Halogenated compounds from China. *Geophysical Research Letters*, 37(12),  
639 2010GL043263. <https://doi.org/10.1029/2010GL043263>
- 640 Li, J., Wang, J., Li, H., Rao, Z., Li, Q., & Luo, S. (2003). The production and release  
641 of CFCs from coal combustion. *Acta Geologica Sinica-English Edition*, 77(1),  
642 81–85. <https://doi.org/10.1111/j.1755-6724.2003.tb00113.x>
- 643 Li, J., Wang, J., Yao, Z., Li, H., Li, Q., Luo, S., et al. (2004). Production and Emission  
644 of Chlorofluorocarbons during Coal Combustion. *Rock and Mineral Analysis*, 23  
645 (1), 1–5. (In Chinese) <https://doi.org/10.15898/j.cnki.11-2131/td.2004.01.001>



- 646 Lickley, M., Fletcher, S., Rigby, M., & Solomon, S. (2021). Joint inference of CFC  
 647 lifetimes and banks suggests previously unidentified emissions. *Nature*  
 648 *Communications*, 12(1), 2920. <https://doi.org/10.1038/s41467-021-23229-2>
- 649 Liu, F., Zhang, Q., Tong, D., Zheng, B., Li, M., Huo, H., et al. (2015). High-resolution  
 650 inventory of technologies, activities, and emissions of coal-fired power plants in  
 651 China from 1990 to 2010, *Atmospheric Chemistry and Physics*, 15, 13299–13317.  
 652 <https://doi.org/10.5194/acp-15-13299-2015>
- 653 Liu, Y., Weng, W., Zhang, Q., Li, Q., Xu, J., Zheng, L., et al. (2024). Ozone-depleting  
 654 substances unintendedly emitted from iron and steel industry: CFCs, HCFCs,  
 655 halons and halogenated very short-lived substances. *Journal of Geophysical*  
 656 *Research: Atmospheres*, 129(17), e2024JD041035.  
 657 <https://doi.org/10.1029/2024JD041035>
- 658 Liu, Z., Guan, D., Wei, W., Davis, S. J., Ciais, P., Bai, J., et al. (2015). Reduced  
 659 carbon emission estimates from fossil fuel combustion and cement production in  
 660 China. *Nature*, 524(7565), 335–338. <https://doi.org/10.1038/nature14677>
- 661 Luo, K., Ren, D., Xu, L., Dai, S., Cao, D., Feng, F., & Tan, J. (2004). Fluorine content  
 662 and distribution pattern in Chinese coals. *International Journal of Coal*  
 663 *Geology*, 57(2), 143–149. <https://doi.org/10.1016/j.coal.2003.10.003>
- 664 McCulloch, A., Ashford, P., & Midgley, P. M. (2001). Historic emissions of  
 665 fluorotrichloromethane (CFC-11) based on a market survey. *Atmospheric*  
 666 *Environment*, 35(26), 4387–4397. [https://doi.org/10.1016/S1352-2310\(01\)00249-](https://doi.org/10.1016/S1352-2310(01)00249-7)  
 667 7
- 668 Molina, M. J., & Rowland, F. S. (1974). Stratospheric sink for chlorofluoromethanes:  
 669 chlorine atom-catalysed destruction of ozone. *Nature*, 249(5460), 810–812.  
 670 <https://doi.org/10.1038/249810a0>
- 671 Montzka, S. A., Dutton, G. S., Yu, P., Ray, E., Portmann, R. W., Daniel, J. S., et al.  
 672 (2018). An unexpected and persistent increase in global emissions of ozone-



- 673 depleting CFC-11. *Nature*, 557(7705), 413–417. [https://doi.org/10.1038/s41586-](https://doi.org/10.1038/s41586-018-0106-2)  
 674 018-0106-2
- 675 Montzka, S. A., Dutton, G. S., Portmann, R. W., Chipperfield, M. P., Davis, S., Feng,  
 676 W., et al. (2021). A decline in global CFC-11 emissions during 2018–2019.  
 677 *Nature*, 590(7846), 428–432. <https://doi.org/10.1038/s41586-021-03260-5>
- 678 National Bureau of Statistics of China, 2000–2021. China energy statistical yearbook  
 679 2001–2022. China Statistics Press, Beijing. From  
 680 <http://cnki.nbsti.net/CSYDMirror/Trade/yearbook/single/N2022060061?z=Z024>
- 681 Niu, Z., Kong, S., Yan, Q., Cheng, Y., Zheng, H., Hu, Y., et al. (2025). Estimation of  
 682 CFC-11 emissions from coal combustion in China, Figshare [data set],  
 683 <https://doi.org/10.6084/m9.figshare.28523063>.
- 684 Palmer, P. I., Jacob, D. J., Mickley, L. J., Blake, D. R., Sachse, G. W., Fuelberg, H. E.,  
 685 et al. (2003). Eastern Asian emissions of anthropogenic halocarbons deduced  
 686 from aircraft concentration data. *Journal of Geophysical Research: Atmospheres*,  
 687 108(D24), 2003JD003591. <https://doi.org/10.1029/2003JD003591>
- 688 Pan, Y., Birdsey, R. A., Fang, J., Houghton, R., Kauppi, P. E., Kurz, W. A., et al.  
 689 (2011). A large and persistent carbon sink in the world's forests. *Science*,  
 690 333(6045), 988–993. <https://doi.org/10.1126/science.1201609>
- 691 Park, S., Western, L. M., Saito, T., Redington, A. L., Henne, S., Fang, X., et al. (2021).  
 692 A decline in emissions of CFC-11 and related chemicals from eastern China.  
 693 *Nature*, 590(7846), 433–437. <https://doi.org/10.1038/s41586-021-03277-w>
- 694 Peng, L., Zhang, Q., Yao, Z., Mauzerall, D. L., Kang, S., Du, Z., et al. (2019).  
 695 Underreported coal in statistics: A survey-based solid fuel consumption and  
 696 emission inventory for the rural residential sector in China, *Applied Energy*, 235,  
 697 1169–1182. <https://doi.org/j.apenergy.2018.11.043>
- 698 Polvani, L. M., Previdi, M., England, M. R., Chiodo, G., & Smith, K. L. (2020).  
 699 Substantial twentieth-century Arctic warming caused by ozone-depleting



- 700 substances. *Nature Climate Change*, 10(2), 130–133.  
 701 <https://doi.org/10.1038/s41558-019-0677-4>
- 702 Pons, J., Tope, H., Walter-Terrinoni, H. (2019). Montreal protocol on substances that  
 703 deplete the ozone layer, report of the technology and economic assessment panel  
 704 May 2019, Volume 3: Decision XXX/3 TEAP Task Force Report on Unexpected  
 705 Emissions of Trichlorofluoromethane (CFC-11). United Nations Environment  
 706 Programme: Nairobi, Kenya. From  
 707 <https://ozone.unep.org/science/assessment/teap>
- 708 Rigby, M., Prinn, R. G., O'Doherty, S., Montzka, S. A., McCulloch, A., Harth, C. M.,  
 709 et al. (2013). Re-evaluation of the lifetimes of the major CFCs and CH<sub>3</sub>CCl<sub>3</sub>  
 710 using atmospheric trends. *Atmospheric Chemistry and Physics*, 13(5), 2691–  
 711 2702. <https://doi.org/10.5194/acp-13-2691-2013>
- 712 Rigby, M., Park, S., Saito, T., Western, L. M., Redington, A. L., Fang, X., et al. (2019).  
 713 Increase in CFC-11 emissions from eastern China based on atmospheric  
 714 observations. *Nature*, 569(7757), 546–550. [https://doi.org/10.1038/s41586-019-](https://doi.org/10.1038/s41586-019-1193-4)  
 715 1193-4
- 716 Scientific assessment of ozone depletion: 2018. (2019). Geneva, Switzerland: World  
 717 Meteorological Organization. From <https://csl.noaa.gov/assessments/ozone/2018/>
- 718 Shao, M., Huang, D., Gu, D., Lu, S., Chang, C., & Wang, J. (2011). Estimate of  
 719 anthropogenic halocarbon emission based on measured ratio relative to CO in the  
 720 Pearl River Delta region, China. *Atmospheric Chemistry and Physics*, 11(10),  
 721 5011–5025. <https://doi.org/10.5194/acp-11-5011-2011>
- 722 Shen, G., Ru, M., Du, W., Zhu, X., Zhong, Q., Chen, Y., et al. (2019). Impacts of air  
 723 pollutants from rural Chinese households under the rapid residential energy  
 724 transition. *Nature Communications*, 10(1), 3405. [https://doi.org/10.1038/s41467-](https://doi.org/10.1038/s41467-019-11453-w)  
 725 019-11453-w



- 726 Shen, G., Xiong, R., Tian, Y., Luo, Z., Jiangtulu, B., Du, W., et al. (2022). Substantial  
 727 transition to clean household energy mix in rural households in China. *National*  
 728 *Science Review*, 9(7), nwac050. <https://doi.org/10.1093/nsr/nwac050>
- 729 Shen, H., Luo, Z., Xiong, R., Liu, X., Zhang, L., Li, Y., et al. (2021). A critical review  
 730 of pollutant emission factors from fuel combustion in home stoves. *Environment*  
 731 *International*, 157, 106841. <https://doi.org/10.1016/j.envint.2021.106841>
- 732 Shen, L., Xiang, P., Liang, S., Chen, W., Wang, M., Lu, S., et al. (2018). Sources  
 733 profiles of volatile organic compounds (VOCs) measured in a typical industrial  
 734 process in Wuhan, Central China. *Atmosphere*, 9(8), 297.  
 735 <https://doi.org/10.3390/atmos9080297>
- 736 Shi, J., Deng, H., Bai, Z., Kong, S., Wang, X., Hao, J., et al. (2015). Emission and  
 737 profile characteristic of volatile organic compounds emitted from coke  
 738 production, iron smelt, heating station and power plant in Liaoning Province,  
 739 China. *Science of The Total Environment*, 515–516, 101–108.  
 740 <https://doi.org/10.1016/j.scitotenv.2015.02.034>
- 741 Simpson, I. J., Barletta, B., Meinardi, S., Aburizaiza, O. S., DeCarlo, P. F., Farrukh, M.  
 742 A., et al. (2022). CFC-11 measurements in China, Nepal, Pakistan, Saudi Arabia  
 743 and South Korea (1998–2018): Urban, landfill fire and garbage burning sources.  
 744 *Environmental Chemistry*, 18(8), 370–392. <https://doi.org/10.1071/EN21139>
- 745 Sun, J., Shen, Z., Huang, Y., Cao, J., Ho, S. S. H., Niu, X., et al. (2018). VOCs  
 746 emission profiles from rural cooking and heating in Guanzhong Plain, China and  
 747 its potential effect on regional O<sub>3</sub> and SOA formation. *Atmospheric Chemistry*  
 748 *and Physics Discussion*. <https://doi.org/10.5194/acp-2018-36>
- 749 Sun, J., Shen, Z., Zhang, L., Zhang, Y., Zhang, T., Lei, Y., et al. (2019). Volatile  
 750 organic compounds emissions from traditional and clean domestic heating  
 751 appliances in Guanzhong Plain, China: Emission factors, source profiles, and  
 752 effects on regional air quality. *Environment International*, 133, 105252.  
 753 <https://doi.org/10.1016/j.envint.2019.105252>





- 754 Tao, S., Shen, G., Cheng, H., & Ma, J. (2021). Toward clean residential energy:  
 755 challenges and priorities in research. *Environmental Science & Technology*,  
 756 55(20), 13602–13613. <https://doi.org/10.1021/acs.est.1c02283>
- 757 Tong, D., Zhang, Q., Liu, F., Geng, G., Zheng, Y., Xue, T., et al. (2018). Current  
 758 emissions and future mitigation pathways of coal-fired power plants in China  
 759 from 2010 to 2030, *Environmental Science & Technology*, 52(21), 12905–12914.  
 760 <https://doi.org/10.1021/acs.est.8b02919>, 2018
- 761 Tsinghua University Building Energy Efficiency Research Center, Energy foundation.  
 762 (2024). Constructing a new rural energy system toward carbon neutrality-  
 763 comprehensive report on the governance of rural domestic coal in China.  
 764 Tsinghua University: Beijing, China. (In Chinese) From  
 765 <https://www.ccetp.cn/newsinfo/7604069.html>
- 766 Wan, D., Xu, J., Zhang, J., Tong, X., & Hu, J. (2009). Historical and projected  
 767 emissions of major halocarbons in China. *Atmospheric Environment*, 43(36),  
 768 5822–5829. <https://doi.org/10.1016/j.atmosenv.2009.07.052>
- 769 Wang, M., Li, S., Zhu, R., Zhang, R., Zu, L., Wang, Y., & Bao, X. (2020). On-road  
 770 tailpipe emission characteristics and ozone formation potentials of VOCs from  
 771 gasoline, diesel and liquefied petroleum gas fueled vehicles. *Atmospheric*  
 772 *Environment*, 223, 117294. <https://doi.org/10.1016/j.atmosenv>
- 773 Wang, M., Li, S., Zhu, R., Zhang, R., Zu, L., Wang, Y., et al. (2020). On-road tailpipe  
 774 emission characteristics and ozone formation potentials of VOCs from gasoline,  
 775 diesel and liquefied petroleum gas fueled vehicles. *Atmospheric Environment*,  
 776 223, 117294. <https://doi.org/10.1016/j.atmosenv.2020.117294>
- 777 Wang, S., Su, H., Chen, C., Tao, W., Streets, D. G., Lu, Z., et al. (2020). Natural gas  
 778 shortages during the “coal-to-gas” transition in China have caused a large  
 779 redistribution of air pollution. *Proceedings of the National Academy of Sciences*,  
 780 117(49), 31018–31025. <https://doi.org/10.1073/pnas.2007513117>



- 781 Western, L. M., Vollmer, M. K., Krummel, P. B., Adcock, K. E., Crotwell, M., Fraser,  
782 P. J., et al. (2023). Global increase of ozone-depleting chlorofluorocarbons from  
783 2010 to 2020. *Nature Geoscience*, 16(4), 309–313.  
784 <https://doi.org/10.1038/s41561-023-01147-w>
- 785 Wu, H., Liu, J., Hu, X., He, G., Zhou, Y., Wang, X., et al. (2024). Fewer than 15% of  
786 coal power plant workers in China can easily shift to green jobs by 2060. *One*  
787 *Earth*, 7(11), 1994–2007. <https://doi.org/10.1016/j.oneear.2024.10.006>
- 788 Wu, J., Kong, S., Zeng, X., Cheng, Y., Yan, Q., Zheng, H., et al. (2021). First high-  
789 resolution emission inventory of levoglucosan for biomass burning and non-  
790 biomass burning sources in China. *Environmental Science & Technology*, 55(3),  
791 1497–1507. <https://doi.org/10.1021/acs.est.0c06675>
- 792 Wu, R., & Xie, S. (2017). Spatial distribution of ozone formation in China derived  
793 from emissions of speciated volatile organic compounds. *Environmental Science*  
794 *& Technology*, 51(5), 2574–2583. <https://doi.org/10.1021/acs.est.6b03634>
- 795 Yan, Q., Kong, S., Yan, Y., Liu, H., Wang, W., Chen, K., et al. (2020). Emission and  
796 simulation of primary fine and submicron particles and water-soluble ions from  
797 domestic coal combustion in China. *Atmospheric Environment*, 224, 117308.  
798 <https://doi.org/10.1016/j.atmosenv.2020.117308>
- 799 Yan, Q., Kong, S., Yan, Y., Liu, X., Zheng, S., Qin, S., et al. (2022). Emission and  
800 spatialized health risks for trace elements from domestic coal burning in China.  
801 *Environment International*, 158, 107001.  
802 <https://doi.org/10.1016/j.envint.2021.107001>
- 803 Yan, Y., Yang, C., Peng, L., Li, R., & Bai, H. (2016). Emission characteristics of  
804 volatile organic compounds from coal-, coal gangue-, and biomass-fired power  
805 plants in China. *Atmospheric Environment*, 143, 261–269.  
806 <https://doi.org/10.1016/j.atmosenv.2016.08.052>



- 807 Ye, X. (2018). Study on characteristics of pollutants emission from non-road mobile  
 808 source and biomass boilers on real work conditions. South China University of  
 809 Technology.
- 810 Zeng, L., Dang, J., Guo, H., Lyu, X., Simpson, I. J., Meinardi, S., et al. (2020). Long-  
 811 term temporal variations and source changes of halocarbons in the Greater Pearl  
 812 River Delta region, China. *Atmospheric Environment*, 234, 117550.  
 813 <https://doi.org/10.1016/j.atmosenv.2020.117550>
- 814 Zeng, X., Kong, S., Zhang, Q., Ren, H., Liu, J., Feng, Y., et al. (2021). Source profiles  
 815 and emission factors of organic and inorganic species in fine particles emitted  
 816 from the ultra-low emission power plant and typical industries. *Science of The*  
 817 *Total Environment*, 789, 147966. <https://doi.org/10.1016/j.scitotenv.2021.147966>
- 818 Zhang, Y., Li, C., Yan, Q., Han, S., Zhao, Q., Yang, L., et al. (2020). Typical industrial  
 819 sector-based volatile organic compounds source profiles and ozone formation  
 820 potentials in Zhengzhou, China. *Atmospheric Pollution Research*, 11(5), 841–850.  
 821 <https://doi.org/10.1016/j.apr.2020.01.012>